
This item was submitted to [Loughborough's Research Repository](#) by the author.
Items in Figshare are protected by copyright, with all rights reserved, unless otherwise indicated.

An evacuated enclosure design for solar thermal energy applications

PLEASE CITE THE PUBLISHED VERSION

PUBLISHER

© Grand Renewable Energy

VERSION

SMUR (Submitted Manuscript Under Review)

PUBLISHER STATEMENT

This work is made available according to the conditions of the Creative Commons Attribution-NonCommercial-NoDerivatives 4.0 International (CC BY-NC-ND 4.0) licence. Full details of this licence are available at:
<https://creativecommons.org/licenses/by-nc-nd/4.0/>

LICENCE

CC BY-NC-ND 4.0

REPOSITORY RECORD

Henshall, Paul, Roger Moss, Farid Arya, Philip C. Eames, Stan Shire, and Trevor Hyde. 2019. "An Evacuated Enclosure Design for Solar Thermal Energy Applications". figshare. <https://hdl.handle.net/2134/16098>.

AN EVACUATED ENCLOSURE DESIGN FOR SOLAR THERMAL ENERGY APPLICATIONS

Paul. Henshall¹, Roger. Moss², Farid. Arya³, Philip. Eames¹, Stan. Shire² and Trevor. Hyde³

¹Centre for Renewable Energy Systems Technology, Loughborough University, UK

²School of Engineering, University of Warwick, UK

³School of the Built Environment, University of Ulster, UK

Flat-plate solar thermal collector technology when coupled with vacuum enclosure technology has potential to supply clean energy efficiently for use in applications including residential water and space heating. This paper focuses on the design of vacuum enclosures for flat-plate solar collectors with specific reference to vacuum enclosures designed for thin micro-channel solar absorber plates (thickness < 10mm). The expectations, requirements and applications of these solar collectors are discussed along with a description of an enclosure concept under consideration. Potential seal materials are identified and their limitations discussed. Finite element modelling results are presented and conclusions made regarding design parameter selection.

Keywords: renewable energy, solar thermal, vacuum

INTRODUCTION

Solar thermal collectors conventionally come in two forms; these being non-evacuated, glazed, flat-plate (FP) collectors and evacuated tube (ET) collectors. FP collectors typically exhibit superior optical performance compared with ET collectors but their thermal performance is worse, especially at elevated temperatures. FP collectors lose heat both by convection of the internal air (or gas) and conduction through it; these modes of heat loss are impossible in a vacuum. Research in solar thermal collectors is therefore seeking to combine the benefits of ET and FP collectors [1]. There are various examples of successfully demonstrated low pressure flat-plate solar collectors in the literature, such as the work by Benz and Beikircher [2], who successfully demonstrated a prototype flat-plate solar collector for process steam production with the collector interior filled with a low pressure krypton gas to reduce convective heat loss. Moreover, a number of vacuum flat-plate solar collectors are becoming commercially available. It is anticipated that a vacuum flat-plate (VFP) solar collector will exhibit greater efficiencies at higher temperatures in comparison to both ET and FP collectors. Acknowledgements: Research funded by the EPSRC.

Background

The concept of employing an evacuated or low pressure enclosure to enhance the thermal performance of flat-plate solar collectors is a concept which dates back to the 1970s [3]. At this time flat-plate solar collectors were limited in their achievable performance; with efficiencies usually less than 40% for absorber plate temperatures greater than 100°C. Eaton and Blum [3] suggest that the use of only a moderate vacuum environment (~150 – 3,500 Pa) between the absorber plate and enclosure glass cover is sufficient to allow the collector to efficiently operate at temperatures exceeding 150°C. Achieving higher temperatures would allow flat plate collectors to be considered for process heat applications. The moderate vacuum pressure range, while being sufficient to effectively suppress convective heat transfer between the absorber plate and the collector glass, still allows for gas conduction heat transfer to take place. Gas conduction can account for several Watts of total power loss from a solar collector [2]. Subsequently, it is desirable to attain a vacuum pressure between the plate and glass cover of less than 0.1 Pa in order to fully suppress both convection and gas conduction

processes and maximize collector thermal performance.

Attaining and maintaining enclosure pressures below 0.1 Pa for an adequate product lifetime represents a significant engineering challenge for a FP collector geometry. This is especially the case when the vacuum layer volume is very small; as in the case of vacuum glazing, which typically employs vacuum layers less than 0.5mm thick [4]. To this end, the design of the evacuated enclosures should protect the glass cover and sealing material from the large stresses imposed by atmosphere pressure forces and stresses due to differential thermal expansion between the various enclosure components.

CONFIGURATION AND PERFORMANCE

Conventional flat-plate solar collectors are typically configured as depicted in figure 1.

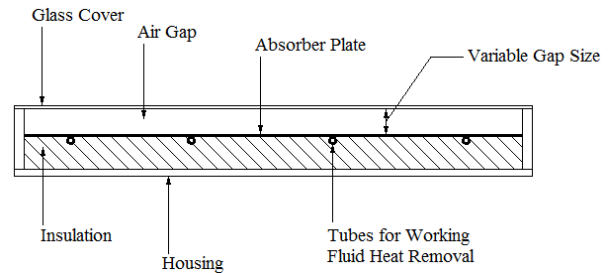


Fig. 1. Conventional configuration of a FP collector [3]

As can be observed in figure 1, the absorber plate and heat removal tubes are insulated on the rear side of the collector with an air gap between the absorber and glass cover on the front side. For such collectors convective heat loss between the absorber and glass cover can be significant. Typically, heat loss from the collector is characterized by the collector overall loss coefficient (U_L), where U_L is calculated as:

$$U_L = U_t + U_b + U_e \quad (1)$$

where U_t is the top loss coefficient, U_b is the back loss coefficient and U_e is the edge loss coefficient (see figure 2). The VFP configuration under consideration in this paper is depicted in figure 2:

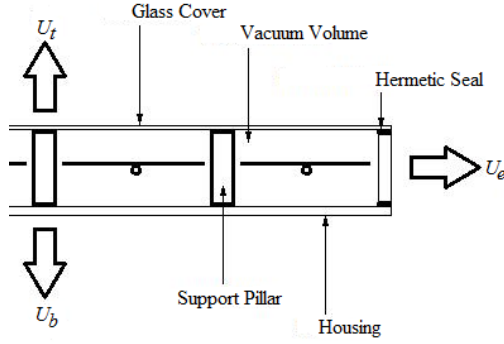


Fig. 2. VFP configuration

In this VFP configuration the absorber plate is suspended within the housing such that it is completely surrounded by vacuum, suppressing convective heat loss. An array of support pillars is required to allow the glass cover and housing to resist atmospheric pressure loading resulting from the evacuated volume within the collector. In this VFP configuration it is expected that U_t will be similar in magnitude to U_b with only radiative heat transfer occurring between the absorber plate and glass cover/back housing. Subsequently, a large decrease in heat loss is expected, resulting in the VFP collector being capable of operating efficiently at higher temperatures.

Using a 1-D flat-plate solar collector modelling methodology, as described by [5], values of heat loss coefficients were estimated for both configurations (FP and VFP) of collector as shown in table 1. For the VFP collector, it should be noted that these values represent an ideal case with only radiative losses directly from the absorber plate present. The general characteristics of the two configurations were based on the Kingspan Solarmax FN 2.0 flat-plate collector [6], for which an air gap of 28mm and a glass cover emissivity of 0.91 are assumed. Furthermore, it is assumed that U_e for the VFP configuration is negligible and the absorber plate emissivity is ~ 0.1 on average. Subsequently, both configurations were modelled and efficiency curves plotted as shown in figure 3.

Table 1: Estimated Heat Loss Coefficients for FP and VFP collectors at $t_m = 140^\circ\text{C}$

| Heat Loss Coefficient | FP | VFP |
|------------------------------------|-----|-----|
| U_t ($\text{W/m}^2 \text{ K}$) | 4.6 | 1.0 |
| U_b ($\text{W/m}^2 \text{ K}$) | 0.4 | 1.0 |
| U_e ($\text{W/m}^2 \text{ K}$) | 0.4 | - |
| U_L ($\text{W/m}^2 \text{ K}$) | 5.4 | 2.0 |

In figure 3, the 1-D FP model performance of the FN 2.0 collector is plotted [6]. As can be seen in figure 3 the 1-D FP model is consistent with manufacturer performance. When using the same model, except with heat loss coefficients as estimated in table 1 for a VFP collector, much greater efficiencies are observed at higher average absorber plate temperatures (t_m). From this analysis it is estimated that a VFP collector could potentially operate with efficiencies greater than 50% at mean plate temperatures up to 120°C . This suggests that a VFP collector is suitable for a wide range of applications such as domestic hot water/space heating and process heat production. For domestic hot water/space heating a VFP collector could efficiently provide heat up to $\sim 100^\circ\text{C}$ to a suitable heat storage system. There is also potential for improved performance through use of optimal material properties and system design. Further work is underway to more accurately simulate the behaviour of such collectors.

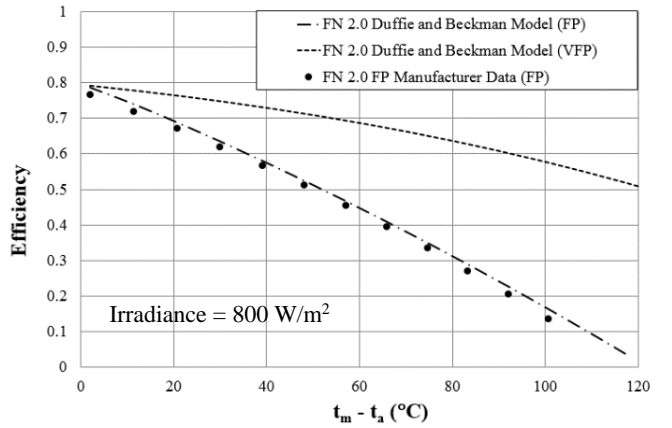


Fig. 3: Efficiency curves for FP, ET and VFP collectors (Ambient temperature (t_a) is 20°C)

The vacuum insulation layer within the enclosure and surrounding the solar absorber can be very thin whilst still remaining effective; thus allowing the collector itself to be only slightly deeper than the depth of the solar absorber plate, as no bulky backing insulation is required. A thin, light weight collector could be easily mounted onto existing roof structures or as a fascia on residential/industrial buildings. For process heat applications VFP collectors could provide heat up to 150°C at competitive efficiencies. This would satisfy several industrial heating requirements such as chemical heat treatments and industrial steam washing [7]. Furthermore, VFP collectors could provide this level of performance without the need for a solar concentrator and associated tracking systems.

HERMETIC SEALING MATERIALS

A contiguous and robust hermetic seal is required between the glass cover and the collector housing to maintain the vacuum within a VFP collector over its lifetime. This type of sealing is akin to that in vacuum glazing, for which there are several candidate materials [4]. A primary factor in the selection of candidate materials is the seal material softening temperature. If the softening temperature is in the range $300\text{--}400^\circ\text{C}$ or higher, then there is a significant likelihood that a tempered glass cover would lose temper during the sealing process and low-emissivity coatings applied to the glass cover may degrade [4]. If the softening temperature of the seal material is relatively low in comparison to the stagnation temperature of the solar collector (200°C in the case of Solarmax) then there is a significantly higher risk that the seal will fail over the product lifetime unless a complicated control system monitors the collector seal temperature. Conventional materials which have been considered for vacuum glazing include solder glass and indium solder alloys [4].

Low temperature solder glass typically has a relatively high softening temperature ($\sim 450^\circ\text{C}$) in comparison to indium and tin based solder alloys. However, in recent years Hitachi has developed a solder glass with a much lower softening temperature from $220\text{--}300^\circ\text{C}$ [8]. The technique for sealing with solder glass involves applying a solder glass paste around the edge of the assembled enclosure which is then placed in an oven to be baked at a temperature greater than the softening temperature of the solder glass. The basic process for using solder glass is discussed in [4].

Indium solder has a softening temperature of approximately $150\text{--}160^\circ\text{C}$ and is bonded to glass and metal surfaces via ultra-

sonic soldering. The sealing technique involves placing two indium coated surfaces together and baking at temperatures up to 170°C. At this temperature the indium is able to sub-duct the surface oxide layer at the joint interface resulting in mixing of the indium bonded to the two components forming a seal between them. This technique, as described in [4], works well for vacuum glazing. However, indium would pose a greater risk of seal failure, due to its low melting point, for a VFP collector. This is especially true around the inlet and outlet ports of the collector. Nonetheless, assuming that the collector stagnation temperature is low enough and the seal is thermally insulated from the flat plate absorber, indium is a feasible seal material.

A range of tin based solders are also considered for this application. One such solder is S-bond 220M, which is a solder alloy consisting of tin, titanium, silver and magnesium [9]. This particular alloy has a softening temperature from 240 - 260°C. The sealing technique is similar to that of indium, however, tin based solders also require surface dross skimming and mechanical activation to break down the surface oxide layer to form the seal; thus further complicating the sealing process.

EVACUATED ENCLOSURE DESIGN CONSTRAINTS

A variety of evacuated enclosure concepts are under consideration in this research project. Currently, the primary concept takes a form similar to that of vacuum glazing with front and back glass covers separated by a metal spacer and a square array of metal support pillars (see figure 4).

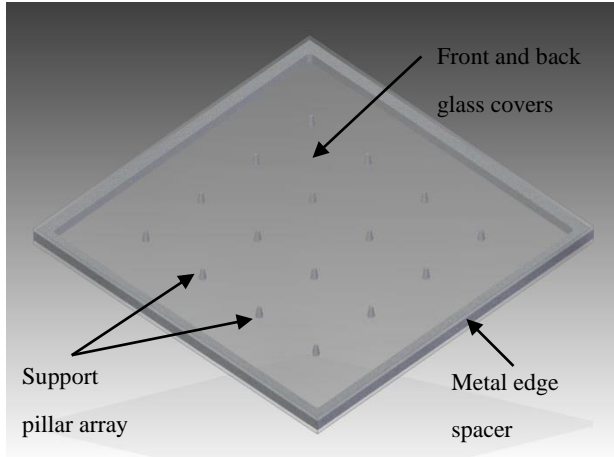


Fig. 4. Evacuated Enclosure Concept

Pillar Array Constraints:

As the evacuated enclosure concept seen in figure 4 is similar to vacuum glazing configurations, many of the design constraints for vacuum glazing are transferable. These constraints include limits on: external glass cover surface tensile stress, internal glass cover stresses for the prevention of Hertzian cone fractures and compression forces on the support pillars; all of which are induced via atmospheric pressure loading. These constraints are met by careful selection of support pillar array parameters, which include support pillar radius (a) and support pillar spacing (λ).

A conservative limit on the glass cover external stress is given by [10] and should not exceed ~4MPa for 4mm annealed glass. Tempered glass is expected to be approximately 5× stronger than annealed glass and therefore shouldn't be exposed

to external tensile stresses exceeding ~20MPa. External tensile stress on the glass is determined via a parametric analysis in which finite element method (FEM) software (Abaqus) is employed to model the stresses in the vacuum enclosure. Limits on internal glass cover stresses for the prevention of Hertzian fractures can be found when considering Auerbach's law; which is discussed by Fischer-Cripps and Collins in [11]; in relation to vacuum glazing. It is important to also consider the compressive stress in the support pillars themselves. The vacuum enclosure support pillar array size and spacing should be selected such that the compressive stress (σ) on the pillars does not exceed the compressive strength of the pillar material. The relationship between pillar separation and pillar radius for a given compressive stress is given by:

$$q\lambda^2 = \sigma\pi a^2 \quad (2)$$

where q is the atmospheric pressure load. If the pillars were very long and thin, one would also need to consider the possibility of failure due to buckling. A final constraint identified specifically for VFP collectors is a limit on total pillar array area such that a large proportion of area is available within the vacuum enclosure for the collector absorber plate to occupy. In the current study, this limit on pillar array area is set to 3% of the available area in the collector.

When considering all these mechanical design criteria, a range of safe values for a and λ can be identified graphically similar to the procedure described by [10].

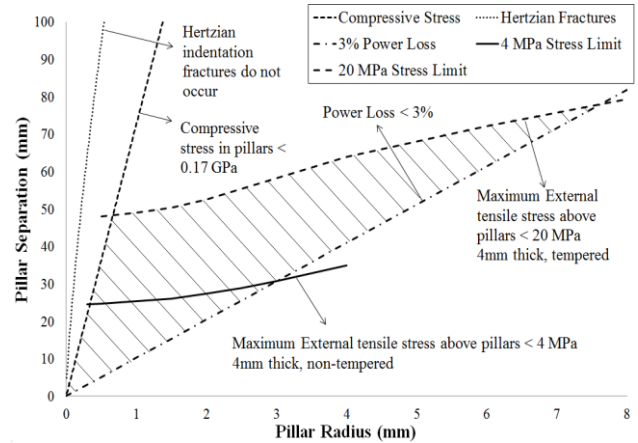


Fig 5: Pillar Radius vs. Pillar Separation for constraints

In figure 5, acceptable combinations of the design parameters (a, λ) can be found within the shaded region bound by the various constraint curves. From figure 5, maximum values of a, λ are found for both annealed and tempered glass (table 2). It should be noted that these analyses are representative of stresses in the centre of the panel. Induced stresses close to inlet/outlet ports will require a more complex analysis.

Table 2: Maximum values of pillar array parameters

| 4mm Thick Glass | Pillar Radius | Pillar Separation |
|-----------------|---------------|-------------------|
| Annealed | 3mm | 31mm |
| Tempered | 7.5mm | 78mm |

Differential Thermal Expansion:

Stresses are also induced in the enclosure due to differential thermal expansion. The seal material between glass cover and

collector housing solidifies, necessarily, at a temperature above those that could possibly be reached in service. Cooling below this stress-free solidification temperature leads to thermally-induced stresses unless the glass, collector housing and seal have identical expansion coefficients. Typically, a metallic edge seal fabricated from aluminium or 300-series stainless steel will have a higher expansion coefficient than soda-lime glass: as it cools, shear stresses across the interface between the materials act at each corner to stretch the metal and compress the glass. This predicates the choice of materials with similar expansion coefficients, a low solidus temperature for the solder and/or a very strong solder.

Chen et al [12] obtained an analytical 2-D solution for thermal stresses, demonstrating that it is only the deformation of the end faces that relaxes the shear stress from a state of infinite stress acting over an infinitesimal length; the central region being free of shear stresses across the interface. This leads to the counter-intuitive result that “increasing the length of the beams has no influence on the distribution of thermal stresses, except that the ‘middle portions’ become longer” [12]

An accurate simulation requires 3D FEM (e.g. Abaqus) but an approximate solution (Figure 6) can easily be achieved using Matlab's Partial Differential Equation toolbox and provides some insight into the stresses acting through the metal-glass interface. The plane stress equations are solved in two dimensions; Duhamel's Analogy [13] is used to represent the thermal expansions via the application of surface stresses to the edges of the grid. This is only an approximation because the Plane Stress condition is not representative of the 3D case and because in Matlab one can only impose stresses to the external grid edges and not to the glass-metal interface.

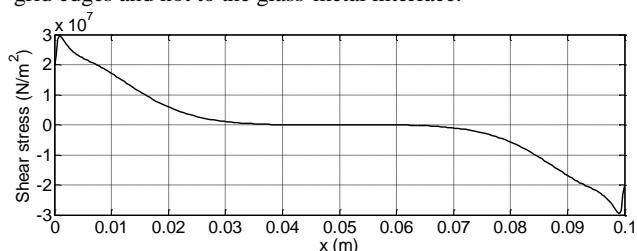


Fig 6: Shear stress across a 2D laminated joint

In figure 6 an approximate solution (2D plane stress) is plotted showing the differential thermal expansion shear stress profile of a 20mm deep aluminium spacer bonded to 5mm thick glass covers at 100°C below the stress-free temperature. Further research is required to determine the suitability of the various seal and enclosure materials to withstand differential thermal expansion stresses in service.

EVACUATED ENCLOSURE FABRICATION

At the University of Ulster work is underway to fabricate this configuration of vacuum enclosure. An example of such an enclosure is seen in figure 7. In this case the enclosure measures 400x400mm, with an aluminium spacer separating front and back glass covers. The seal material bonding metal to glass is indium. The stainless steel pillars are 3mm in radius and spaced at 50mm. Before evacuation the U-value of the enclosure, as a glazing, was ~2.23 W/m²K and after successful evacuation to ~0.001 Pa the U-value was found to be ~0.86 W/m²K; indicating the successful retention of vacuum. It should be noted that a portion of this U-value is due to conduction through the support pillar array. Furthermore, the enclosure is observed to be capable

of withstanding mechanical stresses induced via atmospheric pressure loading and differential thermal expansion.

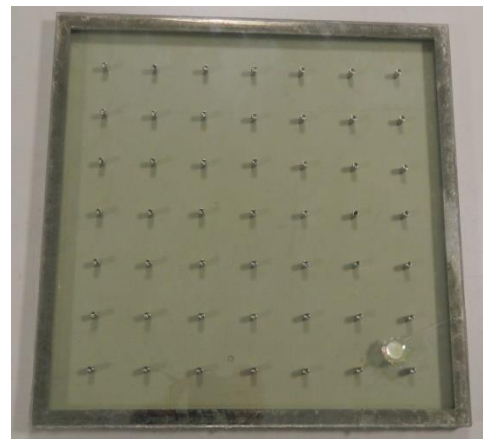


Fig 7: 400x400mm fabricated vacuum enclosure

REFERENCES

- [1] E. Zambolin and D. Del Col, “Experimental analysis of thermal performance of flat plate and evacuated tube solar collectors in stationary standard and daily conditions”, *Solar Energy*. **84**, 2010, pp. 1382-1396.
- [2] N. Benz and T. Beikircher, “High efficiency evacuated flat-plate solar collector for process steam production”, *Solar Energy*. **65**, 1999, pp. 111-118.
- [3] C. Eaton and H. Blum, “The use of moderate vacuum environments as a means of increasing the collection efficiencies and operating temperatures of flat-plate solar collectors”, *Solar Energy*. **17**, 1975, pp 151-158.
- [4] P. Eames, “Vacuum glazing, current performance and future prospects”, *Vacuum*. **82**, 2008, pp 717-722.
- [5] J. Duffie and W. Beckman, *Solar Engineering of Thermal Processes*, 3rd Edition, Wiley, 2006.
- [6] Thermomax technical design guide, Kingspan
- [7] S. Kalogirou, “The potential of solar industrial process heat applications”, *Applied Energy*, **76**, 2003, pp. 337-361.
- [8] Hitachi, “220-300°C low-melting glass for hermetic sealing”, 2012, Press release
- [9] S-Bond Technologies, < <http://www.s-bond.com/products/>>, 2014.
- [10] R. Collins and A. Fischer-Cripps, “Design of support arrays in flat evacuated windows”, *Australian Journal of Physics*. **44**, 1991, pp 545-63.
- [11] A. Fischer-Cripps, “The probability of Hertzian fracture”, *Journal of Materials Science*, vol. **29**, 1994, pp. 2216-2230.
- [12] D. Chen, Thermal stresses in laminated beams, *Journal of Thermal Stresses*, vol. **5**, issue 1, Jan 1982
- [13] S.S. Manson, *Thermal stress and low-cycle fatigue*, McGraw-Hill, 1966